Zayed University
ZU Scholars

All Works

2-27-2024

Camel Dung-Derived Biochar for the Removal of Copper(II) and Chromium(III) Ions from Aqueous Solutions: Adsorption and Kinetics Studies

Kenesha Wilson
Zayed University, kenesha.wilson@zu.ac.ae

Jibran Iqbal
Zayed University, jibran.iqbal@zu.ac.ae

Amira Obaid Abdalla Obaid Hableel
Zayed University

Zainab Naji Khalaf Beyaha Alzaabi
Zayed University

Yousef Nazzal
Zayed University, yousef.nazzal@zu.ac.ae

Follow this and additional works at: https://zuscholars.zu.ac.ae/works

 Part of the Life Sciences Commons

Recommended Citation

Wilson, Kenesha; Iqbal, Jibran; Hableel, Amira Obaid Abdalla Obaid; Alzaabi, Zainab Naji Khalaf Beyaha; and Nazzal, Yousef, "Camel Dung-Derived Biochar for the Removal of Copper(II) and Chromium(III) Ions from Aqueous Solutions: Adsorption and Kinetics Studies" (2024). *All Works*. 6427.
https://zuscholars.zu.ac.ae/works/6427

This Article is brought to you for free and open access by ZU Scholars. It has been accepted for inclusion in All Works by an authorized administrator of ZU Scholars. For more information, please contact scholars@zu.ac.ae.

ACS OMEGA

Open Access

This article is licensed under CC-BY-NC-ND 4.0

http://pubs.acs.org/journal/acsodf

Article

Camel Dung-Derived Biochar for the Removal of Copper(II) and Chromium(III) Ions from Aqueous Solutions: Adsorption and Kinetics Studies

Kenesha Wilson,* Jibran Iqbal, Amira Obaid Abdalla Obaid Hableel, Zainab Naji Khalaf Beyaha Alzaabi, and Yousef Nazzal

Cite This: *ACS Omega* 2024, 9, 11500−11509

Read Online

ACCESS | Metrics & More | Article Recommendations

ABSTRACT: This study explores an innovative approach to tackle the critical issue of heavy metal ion contamination in aqueous solutions through the utilization of camel dung-derived biochar. In the context of global environmental concerns and the adverse impacts of heavy metal pollution on ecosystems and human health, the investigation focuses on copper(II) and chromium(III) ions, which are among the most pervasive pollutants originating from industrial activities. The research revealed that camel dung-derived biochar exhibits exceptional potential for the removal of copper(II) and chromium(III) ions, with removal efficiencies of more than 90% and adsorption capacities of 23.20 and 23.36 mg/g, respectively. The adsorption processes followed second-order kinetics, and the data fitted both the Langmuir and Freundlich adsorption models. The underlying mechanisms governing this adsorption phenomenon seem to be grounded in complexation reactions, cation exchange, and cation−π interactions, underscoring the multifaceted nature of the interactions between the biochar and heavy metal ions. This research not only advances our understanding of sustainable materials for water purification but also harnesses the underutilized potential of camel dung as a valuable resource for environmental remediation, offering a promising avenue for addressing global water pollution challenges.

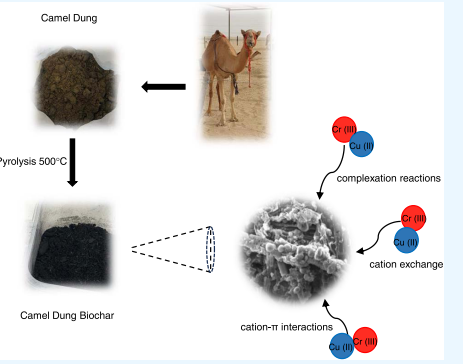

INTRODUCTION

Heavy metal ion-induced water pollution has emerged as a global concern, particularly due to significant levels detected in industrial wastewater, posing hazardous effects on both the environment and human health.[1] Copper (Cu II) and chromium (Cr III) ions are prominent pollutants that originate from industrial activities, such as mining, electroplating, and tanning. Recent reports have highlighted a substantial presence of Cr (III) in wastewater from dental clinics, further emphasizing the diverse sources contributing to the contamination of water bodies with these pollutants.[2] Cr (III) is important for metabolism in mammals; however, if present in high concentrations in aqueous media, it may result in increased incidences of cancer as its +3 oxidation state is very common in normal ecological situations.[3] To mitigate the risk of chromium-(III) oxidation to the more toxic hexavalent chromium, it is imperative to rigorously limit and control overall chromium emissions.[4] Copper, considered an essential nutrient, can turn into a drinking water contaminant due to its nonbiodegradability, extreme toxicity, accumulation tendencies, and widespread sources.[5] Compounds like copper sulfate, found in certain contexts, can lead to health issues, including respiratory, renal, hemolytic, and gastrointestinal disorders.[6]

The presence of these metal ions in aquatic ecosystems can lead to harmful effects on aquatic life, bioaccumulation in the food chain, and long-term human health risks.[7−9] Therefore, there has been growing interest in the development of eco-friendly and sustainable approaches for the removal of these heavy metal ions from contaminated waters. Among these, biochar, a carbon-rich material derived from the pyrolysis of organic matter, has emerged as a promising adsorbent due to its exceptional properties. Some of these properties include adsorption capabilities, easy recovery, low cost, easy availability, and abundance of various functional groups, such carboxyl, hydroxyl, and phenolic groups.[5,10,11] Biochar preparation and use has been shown to be an evolving biotechnology application owing to its ability to immobilize both inorganic and organic contaminants from the environment[12,13] and enhance soil

Received: October 26, 2023
Revised: January 27, 2024
Accepted: January 31, 2024
Published: February 27, 2024

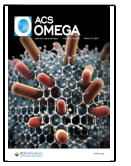

Downloaded via 195.229.148.135 on March 26, 2024 at 10:24:18 (UTC).
See https://pubs.acs.org/sharingguidelines for options on how to legitimately share published articles.

ACS Publications

© 2024 The Authors. Published by American Chemical Society

https://doi.org/10.1021/acsomega.3c08230
ACS Omega 2024, 9, 11500−11509

fertility, carbon sequestration, and environmental remediation.[14]

The utilization of animal manure as a precursor for biochar production has garnered significant attention, offering the dual advantages of waste management and pollutant remediation. Animal manure is abundantly available as an agricultural byproduct, making it an attractive feedstock for biochar production. It possesses inherent properties that contribute to the effectiveness of biochar as an adsorbent, including a high carbon content, abundant surface functional groups, and a diverse mixture of organic compounds.[5,10,15] Furthermore, biochar production from animal manure provides a sustainable approach to managing this waste stream, reducing greenhouse gas emissions, and minimizing environmental pollution.

Xu et al.[11] reported that dairy manure-derived biochar was effective in the removal of Cu, Zn, and Cd ions from aqueous solutions. The adsorption of metals by biochar was attributed mainly to the precipitation of metal ions with PO_4^{3-} and CO_3^{2-} ions in biochar.[16] Mohan et al.[16] asserted that biochar made from cow and pig manure offered excellent adsorption capacity (>88 mg/g) for Cu (II) metal ions. The same study also reported that dairy, pig, and cow manure biochars were able to remove more than 200 mg/g of Pb (II), the highest amount of removal when compared to other types of biochar prepared from materials such as pine wood, oak wood, and rice husk. A high adsorption capacity was also reported for pig and cow manure biochars for the adsorption of Cd (II) ions.[16] In a parallel investigation, Meng et al.[10] explored the efficacy of both fresh and aerobically composted swine manures in adsorbing Cu (II) from aqueous solutions. The findings revealed that the biochar derived from composted swine manure, particularly at 400 °C, exhibited superior adsorption capabilities for removing Cu (II) from wastewater compared to the biochar produced from fresh manure.

In an alternative study, Xu et al.[17] examined the efficacy of biochar prepared from the co-pyrolysis of swine manure and corn straw for the adsorption of metal ions such as Ni (II), Cu (II), and Pb (II). Biochar made from chicken manure was also found to be effective for the adsorption of Pb (II) ions from aqueous solutions. In a study by Cuixia et al.,[18] investigating the impact of different pyrolysis temperatures on the removal of Pb (II) ions from aqueous solutions using biochar derived from chicken manure, it was observed that the optimal adsorption capacity occurred within a pH range of 4.5−7.5. This pH range was noted for its ability to enhance the negative charges on the surface of the adsorbent. The study also identified 800 °C as the most effective pyrolysis temperature for adsorbing metal ions. Similarly, Batool et al.[19] evaluated the adsorption efficiency of biochar derived from farmyard and poultry manures for the removal of Cu (II). Notably, both types of biochar exhibited a maximum copper adsorption at a pH of 2.

Additionally, Wang and Liu[12] have reported that modified yak manure had enhanced adsorption capacities for heavy metals such as Pb(II), Cu (II), Cd (II), and Zn (II) ions. The study claimed that the absorption capacity of Pb (II) with yak manure biochar was 76.41 mg/g, and this increased to 169.57 mg/g when yak manure biochar was modified with H_2O_2. The authors suggested that the enhanced adsorption of metal ions resulted from an augmentation of carboxyl and other oxygen-containing groups in yak manure following modification which facilitated more complexation reactions between the modified biochar and the metal ions. In a similar vein, the surface of dairy manure biochar was alkaline-modified, yielding an engineered biochar with significantly improved absorption capacity for Pb (II) and Cd (II) ions.[20]

The literature has shown that the possibility of using animal manure to prepare biochar is viable, although the optimal conditions for the preparation of the biochar and adsorption parameters seem to differ tremendously. This study involves the preparation of camel dung-derived biochar through controlled pyrolysis followed by thorough characterization of its physicochemical properties. The adsorption experiments encompass a systematic preliminary investigation of various parameters, including initial metal ion concentrations, contact time, and pH levels, to evaluate the adsorption efficiency of the biochar. Furthermore, isotherm and kinetic models are employed to elucidate the adsorption mechanisms and predict the maximum adsorption capacities.

There are approximately 450,000 camels in the United Arab Emirates (UAE).[21] An adult drought camel can yield an average of 8−11 kg of dung per day, and this figure increases for dairy camels.[22] On an annual scale, this accumulates to more than 1.3 million tons. However, the current utilization of this waste in the UAE is predominantly limited to small-scale applications, serving mainly as fertilizer for farmers.[23] Recently, there has been an emerging practice of using camel dung as a fuel in a cement factory located in Ras Al Khaimah, one of the emirates in the UAE.[22] Despite these applications, there is a notable scarcity in the existing literature concerning the use of camel dung, specifically as a precursor for the preparation of biochar.

The outcomes of this study therefore have significant implications for both environmental remediation and waste management within the context of the Gulf Region. By utilizing camel dung as a precursor for biochar production, not only can the pollution caused by heavy metal ions be mitigated but also a sustainable waste management solution can be established, reducing the environmental impact of biomass waste.

MATERIALS AND METHODS

Preparation of Sample Solutions. All chemicals utilized in this research were of analytical quality. To create a 1000 mg/L stock solution of the Cr (III) solution, anhydrous chromium chloride ($CrCl_3$) was employed. The stock solution was formulated by dissolving 3.054 g of $CrCl_3$ salt in 1000 mL of deionized water. For pH adjustments, 0.1 mol/L NaOH and 0.1 mol/L HCl were employed. To make the stock solution of Cu (II), a 1000 mg/L stock solution was prepared by dissolving 3.929 g of $CuSO_4$. $5H_2O$ in 1000 mL of deionized water, and subsequent dilutions were made to prepare the working solutions.

Preparation of Biochar from Camel Dung (CDB). Camel dung was obtained from a camel farm in the emirate of Abu Dhabi. Plant particles were removed from the dung, after which it was air-dried. The dung was then dried in an oven at 60 °C for 48 h. The camel dung was then converted into biochar by the process of slow pyrolysis in an electrical muffle furnace set at 500 °C that was maintained for a residence time of 4 h in an oxygen free environment. The biochar produced was left inside the container overnight to cool by free convection. The biochar was then sieved to obtain a particle size between 0.6 and 1.4 mm, and the selected fraction was stored in airtight containers until required for experiments.

Characterization of Biochar. The camel dung biochar surface morphology as well as elemental analysis was determined using scanning electron microscopy and energy-dispersive X-ray spectroscopy (SEM−EDX), with a TESCAN VEGA (LMU

https://doi.org/10.1021/acsomega.3c08230
ACS Omega 2024, 9, 11500−11509

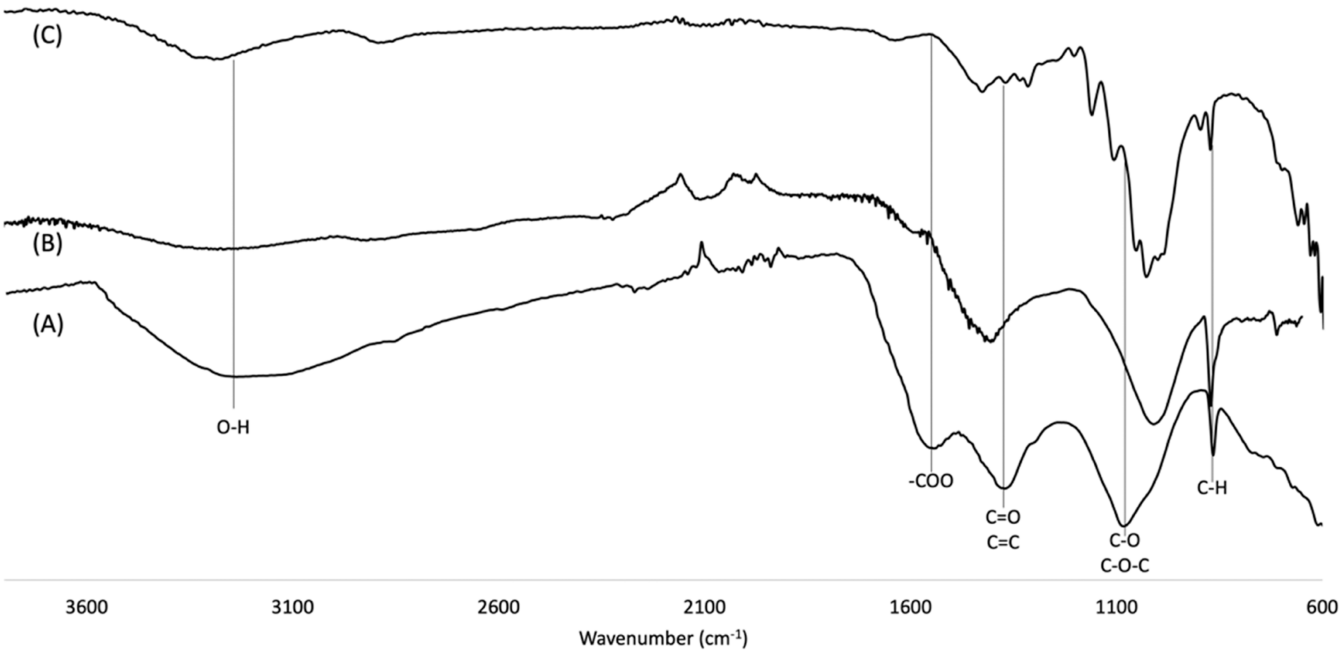

Figure 1. FTIR scan of camel dung biochar, (A) CDB, (B) after the adsorption of Cu (II), and (C) after the adsorption of Cr (III).

INCax-act (Oxford Instruments)) device operating at 20kV. Functional groups on the surfaces of the biochar and biochar after the adsorption of the metal ions were analyzed using Cary 630 Fourier transform infrared spectroscopy (FTIR, Agilent technologies, Danbury, Conn) with a scanning range between 400 and 4000 cm^{-1}. Furthermore, the surface area characteristics of the biochar were assessed through the utilization of a Brunauer−Emmett−Teller (BET) micromeritics analyzer obtained from Micromeritics Instrument Corp (Norcross, GA). The crystallographic properties of both the original biochar and the biochar after metal ion adsorption were investigated using X-ray diffraction analysis (XRD/Rigaku Ultima III) employing a CuKa radiation source (40 kV/30 mA) and a NaI detector.

Batch Adsorption Experiments. Batch adsorption experiments were carried out at room temperature (approximately 22 °C). Further dilution of the stock solution was done to prepare different concentrations of the metal ion solutions ranging in concentrations from 5 to 50 mg/L. Samples were then prepared by mixing 0.1 g of biochar in 50 mL of solutions of different concentrations of metals (5, 10, 20, 30, and 40 mg/L) after which they were agitated on a rotary shaker set at 80 rpm until the time of equilibrium absorption. The pH of these solutions was initially adjusted to between pH 2 and 10. After agitation, the solutions were filtered with 0.45 μm Millipore filters and the residual metal ion concentration was analyzed using an inductively coupled plasma−optical emission spectrometer (ICP-OES, PerkinElmer Avio 200).

The adsorption capacity of each metal ion adsorbed by the biochar and the percentage removal efficiency were determined as shown by the equations below[24]

$$q_e = \frac{(C_o - C_e)V}{m} \tag{1}$$

$$q_t = \frac{(C_o - C_t)V}{m} \tag{2}$$

$$R(\%) = \frac{(C_o - C_e)}{C_i} \times 100 \tag{3}$$

where C_o (mg L^{-1}), C_e (mg L^{-1}), and C_t (mg L^{-1}) are the initial, equilibrium, and concentration after some time, t, of the metal ions, respectively, V is the volume of the metal ion solution (L), m is the mass of biochar used (g), and q_e and q_t are the mass of metal ions adsorbed to the biochar at equilibrium and after time, t.

Modeling of Adsorption Equilibrium and Kinetics. The modeling of metal ion concentrations at equilibrium using Langmuir and Freundlich isotherms was used to ascertain the relationship and interactions between the amounts of adsorbed metal ions and the adsorbate. The Langmuir isotherm assumes uniform monolayer adsorption without interactions between adsorbed molecules, while the Freundlich isotherm describes multilayer adsorption on heterogeneous surfaces, indicating varied binding energies and uneven active site distribution.

The Langmuir equation can be expressed as

$$q_e = \frac{q_m K_L C_e}{1 + K_L C_e} \tag{4}$$

K_L is the adsorption or Langmuir constant (L/mg), q_t is the amount of metal ion adsorbed (mg/g) on the biochar, q_m is the maximum adsorption capacity (mg/g), and C_e the metal ion concentration at equilibrium (mg/L).

The nonlinear form of the Freundlich equation is written as shown in eq 5.

$$q_e = K_F C_e^{1/n} \tag{5}$$

where K_F (mg/g) is the Freundlich constant and n (g/L) is the adsorption heterogeneity factor.

Adsorption kinetics were analyzed using pseudo-first- and pseudo-second-order models, which offer mathematical frameworks to understand the temporal aspects of the adsorption process. The pseudo-first-order model estimates the rate constant and initial adsorption rate, primarily focusing on

https://doi.org/10.1021/acsomega.3c08230
ACS Omega 2024, 9, 11500−11509

early stage behavior. On the other hand, the pseudo-second-order model assumes a proportional relationship between adsorption rate and unoccupied sites. The pseudo-second-order model provides a more comprehensive understanding of the entire adsorption process, including rate constants and maximum adsorption capacities.

Pseudo-first-order (PSO) model can be expressed as eq 6

$$q_t = q_e(1 - e^{-k_1 t}) \quad (6)$$

The nonlinear form of the pseudo-second-order model is written as

$$q_t = \frac{q_e^2 k_2 t}{1 + q_e k_e t} \quad (7)$$

The leaching of Cr (III) and Cu (II) ions was examined by analyzing the desorbed concentrations of the metal ions following washing the solid adsorbent with water. Subsequently, the regenerated adsorbent was employed for the repeated removal of Cr (III) and Cu (II), with the corresponding removal efficiencies assessed at the second run.

RESULTS AND DISCUSSION

The functional groups present in the CDB were analyzed using its FTIR spectra to identify groups that would contribute to the adsorption of heavy metals, as shown in Figure 1.

The results of the FTIR analysis conducted on the biochar made from camel dung before adsorption are presented in Figure 1(A). The signal detected at approximately 3400 cm^{-1} indicates the presence of O−H stretching and suggests the existence of phenols, alcohols, and carboxyl in CBD due to the presence of lignin and hemicellulose.[9,25] The broad peak observed at approximately 1570 cm^{-1} is likely due to −COO asymmetrical stretching of carboxylic acids.[26,27] The peak at 1440−1380 can be attributed to C═O stretching commonly associated ketones and carboxyl structures and C═C vibrations in aromatic rings.[9,27] The bands detected at around 1000 and 1020 cm^{-1} may be attributed to stretches from the bonds C−O and C−O−C.[28] The peak observed at approximately 872 cm^{-1} can be linked to the C−H out-of-plane aromatic bending.[25] The presence of oxygen-containing groups, such as those found in carboxyl and phenolic groups on the surface of the biochar, can act as complexing agents for the adsorption of Cu (II) ions.[9,26,29] The function of these groups in the complexation with Cr (III) has also been reported by Batool et al.[3] FTIR scans in Figure 1 clearly show the presence of these groups on the CDB. After the adsorption of Cu (II) and Cr (III), the intensity of these peaks was either reduced and or shifted slightly, which supports the claim that these groups play a role in complexing Cu (II) and Cr (III) from solutions.

The surface characteristics of the camel dung biochar were studied using a BET surface area analyzer based on the N_2-adsorption−desorption, and the results obtained are given in Figure 2. The results obtained showed that the camel dung biochar exhibits a surface area of 4.4810 cm^2/g, pore volume of 0.006979 cm^3/g, and pore size of 6.23 nm. The obtained isotherm from the N_2-adsorption−desorption of the biochar gave a hysteresis loop which was found to be type IV. The type IV hysteresis loop suggests that the material exhibits a significant mesoporous nature and possibly could lead to high adsorption of the target contaminant[30] with strong adsorbate to adsorbent interactions.[31]

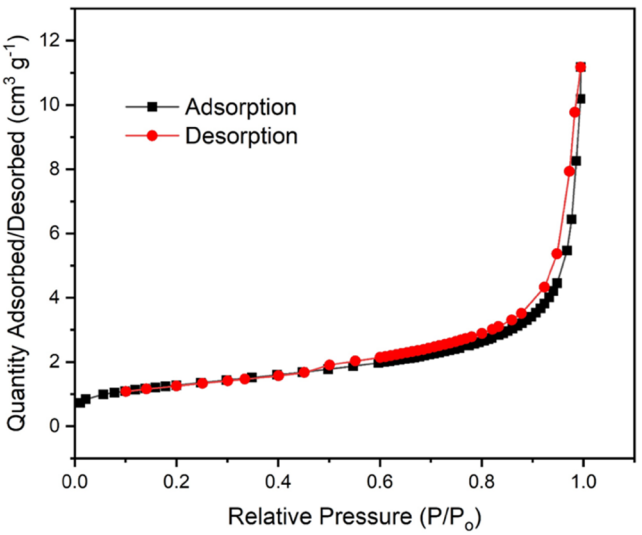

Figure 2. Adsorption−desorption of the N_2 isotherm by CDB.

The surface characteristics of camel dung biochar were assessed through SEM scans, as depicted in Figure 3(A). These scans, complemented by the BET results, affirmed the highly porous nature of the biochar's surface structure. This observation implies a substantial potential for the effective adsorption of metal ions. This finding is consistent with previous research demonstrating that greater porosity and surface area are positively correlated with increased adsorption capacity.[32]

Following metal ion adsorption, SEM scans of the biochar surface were conducted, as shown in Figure 3 (B,C). These scans revealed a highly agglomerated and less porous structure, indicating that metal ions were successfully adsorbed on the biochar surface and had filled in the porous cavities. The EDX analysis spectrum of the CDB showed strong signals for the C, O, Si, Ca, Mg, and K atoms (Figure 3A). Prior to the adsorption of copper (II) and chromium (III), the EDX scan of the CDB did not indicate the presence of copper (II) and chromium (III) ions. Subsequent EDX scans of the biochar (Figure 3B,3C) following the adsorption process clearly identified the presence of chromium (III) and copper (II), respectively, providing evidence of successful adsorption.

Figure 4 illustrates the XRD scans of the CDB both before and after the adsorption process involving Cu (II) and Cr (III) ions.

The XRD scans revealed that the crystalline constituents within the CDB primarily consist of quartz (Q) and calcite (C). The presence of quartz in the biochar is expected since the camel dung was collected from the desert. Following the adsorption of copper (II), discernible peaks emerged, indicating the potential formation of copper sulfate compounds, possibly in the crystalline form of langite (L)—$Cu_4(SO_4)(OH)_6{\cdot}2H_2O$. The observation of this compound post copper adsorption on biochar is similar to findings reported by Wei et al.,[9] who noted similar outcomes in the adsorption of copper on biochar derived from artichoke stalks. Interestingly, the XRD scans did not distinctly identify the chromium compounds. However, this would suggest that these compounds lacked a crystalline nature, particularly given that the EDX scans validated the presence of chromium subsequent to the adsorption process. This nuanced interpretation suggests that while chromium compounds might not have exhibited crystallinity, their existence on the biochar is substantiated by complementary analytical techniques.

https://doi.org/10.1021/acsomega.3c08230
ACS Omega 2024, 9, 11500−11509

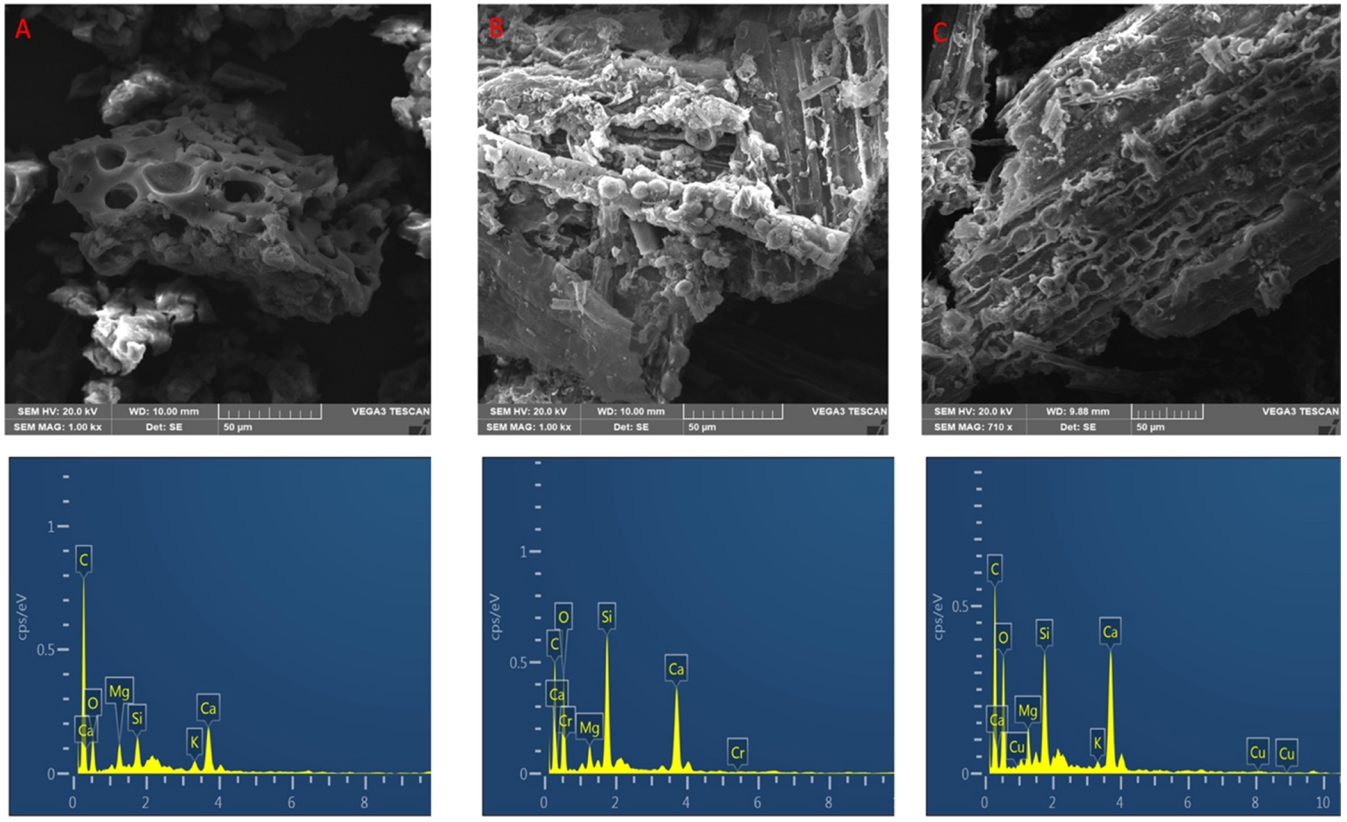

Figure 3. SEM scans and EDX of camel dung biochar (A), camel dung biochar after Cr (III) adsorption (B), and camel dung biochar after Cu (II) adsorption (C).

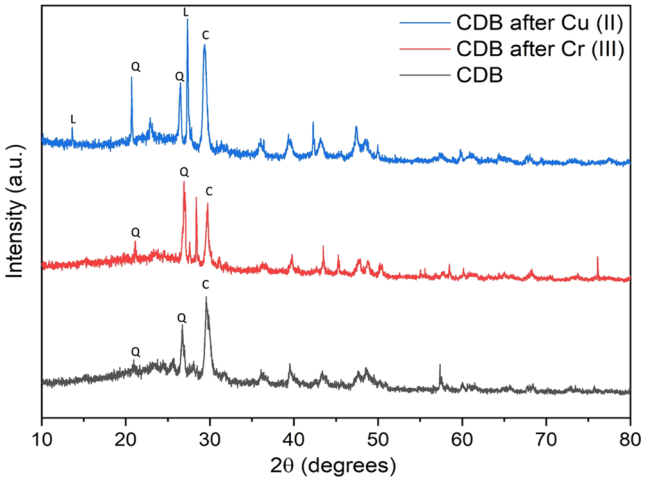

Figure 4. XRD scans of biochar before and after the adsorption of Cu (II) and Cr (III) ions.

Effect of pH on Adsorption. Figure 5 (A) shows the removal efficiency as a factor of pH. Changes in pH did not seem to affect the adsorption process of the metal ions on the CDB. Regardless of the pH, the removal efficiency was approximately 91% for both ions. These results demonstrate that camel dung biochar can be an effective adsorbent without having its pH modified. The pH of the adsorbent material was determined to be approximately 8 and therefore all adsorption experiments were performed without pH modifications. In situations where the adsorption is pH-dependent, it necessitates continuous monitoring and adjustment of pH levels, which can be challenging and time-consuming. In contrast, pH-independent adsorption, such as was determined with the use of CDB, offers operational flexibility by allowing the treatment system to accommodate pH variations without compromising adsorption efficiency.

Effect of Contact Time and Adsorption Kinetic Modeling. The influence of the contact time on the adsorption capacity of CDB is shown in Figure 5 (B). The data suggests that the Cr (III) adsorption occurred rapidly during the initial 1 h, when about 90% of Cr (III) ions were removed. The adsorption of Cu (II) occurred somewhat more slowly, and saturation of the adsorption sites seemed to begin at around the 8 h mark.

To further analyze the efficiency of adsorption, the pseudo-first-order and pseudo-second-order kinetic models were applied to the experimental data (Figure 6). The experimental data for both metal ion solutions fitted the pseudo-second-order model better than the pseudo-first-order model based on the comparison of R^2 values as shown in Table 1. The validity of the pseudo-second-order model is further confirmed, as indicated by the close agreement between the predicted q_e values and the experimental q_e for both Cu (II) and Cr (III) ions adsorbed onto CDB. Prior studies have also documented the applicability of pseudo-second-order adsorption kinetics in the context of Cu (II) and Cr (III) adsorption onto biochar derived from plant and or animal biomass, reinforcing the consistency of these findings within the existing body of literature.[3,4,10,11,33]

Data that follows pseudo-second-order kinetics suggest that adsorption is contingent on the number of vacant binding sites and is controlled by a chemisorption mechanism, or the adsorption process occurs through the sharing or exchange of electrons between the metal ions and those of the CDB.[20] This

https://doi.org/10.1021/acsomega.3c08230
ACS Omega 2024, 9, 11500−11509

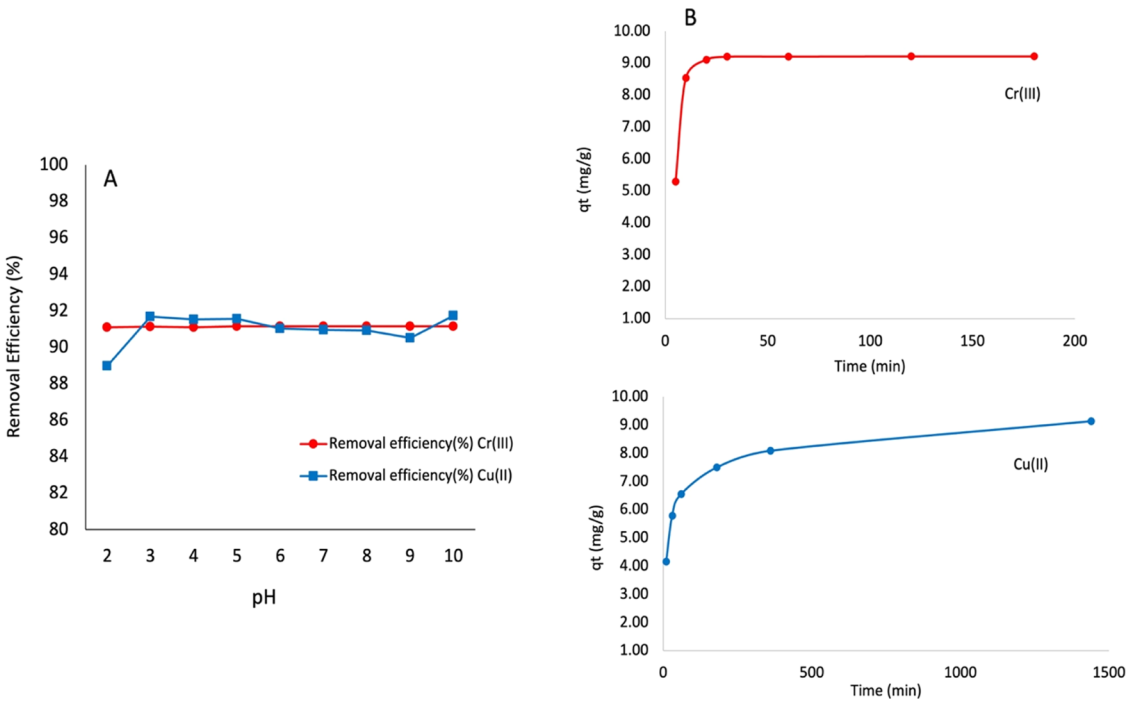

Figure 5. Effect of pH on adsorption efficiency (A) and adsorption kinetics (B) of Cr (III) and Cu (III) on CDB. Concentrations of Cr (III) and Cu (II) were 20 mg/L.

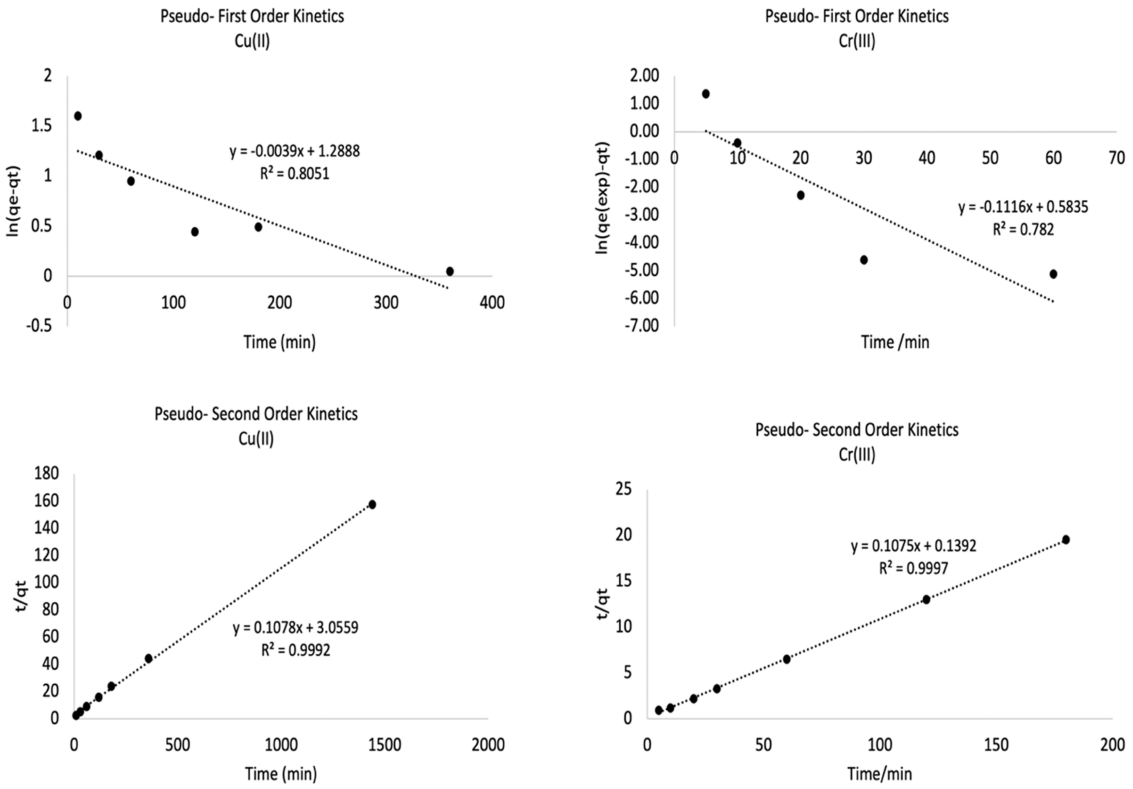

Figure 6. Adsorption Kinetics of Cr (III) & Cu (II) on CDB.

suggests that the adsorption of these metal ions on CDB is effective, making it an attractive option for the removal of contaminants from aqueous solutions.

Effects of Initial Concentrations of Cr (III) and Cu (II) Ions. Figure 7 displays the role of the CDB adsorbent in the removal of different concentrations of Cr (III) and Cu (II), i.e., 5, 10, 20, 30, and 40 mg/L. The results obtained showed that increasing initial concentrations of Cr (III) showed no effect on the removal efficiency. This aligns with reports suggesting that metal ions with fewer available sites for adsorption may not exhibit a significant impact on removal efficiency,[34] which could explain the observed trend in our study for Cr(III). Also, Cr (III)

https://doi.org/10.1021/acsomega.3c08230
ACS Omega 2024, 9, 11500−11509

Table 1. Adsorption Kinetics Parameters for Cu (II) and Cr (III) onto CDB

metal ion	pseudo-first order model		pseudo-second-order model	
Cr (III)	k_1	0.2570	k_2	0.0830
	$q_{e\ (cal)}$	1.7923	$q_{e\ (cal)}$	9.3023
	$q_{e\ (exp)}$	9.2135	$q_{e\ (exp)}$	9.2135
	R^2	0.7820	R^2	0.9997
Cu (II)	k_1	0.0039	k_2	0.0038
	$q_{e\ (cal)}$	3.6284	$q_{e\ (cal)}$	9.2764
	$q_{e\ (exp)}$	9.1395	$q_{e\ (exp)}$	9.1395
	R^2	0.8051	R^2	0.9992

has a smaller ionic radius and consequently could be adsorbed at high concentration. On the contrary, the removal efficiency of Cu (II) demonstrated a decline in adsorption efficiency with increasing initial concentration which is consistent with the results from a previous study.[35] The larger ionic radius of Cu (II) may result in lower concentrations being adsorbed, which further decreases at higher concentrations.

Adsorption Isotherm. Isotherm modeling helps to describe interactions between the adsorbate and the adsorbent. The removal of chromium (III) and copper (II) by CDB was investigated by using the Langmuir and Freundlich adsorption models. The Langmuir model assumes that the thickness of the adsorbed layer is monolayer and that the adsorption process occurs at identical and equivalent localized site with all sites on the adsorbent having an equal affinity for the adsorbate. The Freundlich model defines the heterogeneity and multilayered nature of the surface of the adsorbate.[26] According to the Freundlich model, when the intensity of adsorption or surface heterogeneity factor (n) is greater than 1, the adsorption is favorable.[3,36]

Figure 8 illustrates the plots of both models, demonstrating a strong fit that underscores the complexity of the adsorption behavior in this system. Notably, the Langmuir model exhibits a slightly better fit than the Freundlich model, as reflected in higher R^2 values (Table 2). This aligns with similar studies that have reported a better fit of Cu (II) and Cr (III) adsorption to the Langmuir model when compared to alternative models.[10,11,33,37] The values of $1/n$ (0.7092 for Cr (III) and 0.4159 for Cu (II)) indicate that the adsorption of both metal ions is favorable and nonlinear according to the Freundlich model (Table 2).

The data also shows that the qmax for Cr (III) was close to that for Cu (II); 23.3640 mg/g and 23.2010 mg/g, respectively (Table 2). The similar q_{max} values indicate that both metal ions have comparable maximum adsorption capacities on the adsorbent surface. This suggests that, under ideal conditions, the adsorbent can adsorb a similar amount of both metal ions, and there might be comparable active sites available for adsorption.

Proposed Adsorption Mechanisms. The FTIR scans of the CDB confirmed the presence of oxygen-containing groups, specifically carboxyl and phenolic groups, on the surface of biochar. These groups play a pivotal role in metal ion adsorption, particularly for Cu (II) ions and Cr (III).[3,29] These functional groups possess oxygen atoms with lone pairs that can readily form coordination bonds with metal ions. The complexing ability of carboxyl and phenolic groups lies in their Lewis basic nature, allowing them to act as electron donors during complexation reactions. As Cu (II) and Cr (III) ions approach the biochar surface, the oxygen-containing groups attract and coordinate with these metal ions, forming stable complexes.[9,26] This complexation process enhances the affinity of biochar for Cu (II) and Cr (III), facilitating their adsorption.

Apart from the complexation reactions involving Cu (II) and Cr (III) ions with carboxyl and phenolic groups, the adsorption of Cu (II) and Cr (III) onto biochar may involve cation exchange mechanisms. Specifically, the exchange between Cu and Cr ions and other metal cations, such as Ca^{2+} and Mg^{2+}, associated with surface functional groups in biochar could play a significant role in enhancing the adsorption of Cu (II) and Cr (III). Chen et al.[7] suggested that biochar derived from municipal sludge, containing Ca and Mg adhering to the biochar matrix as cations, undergoes an exchange process with soluble cations,

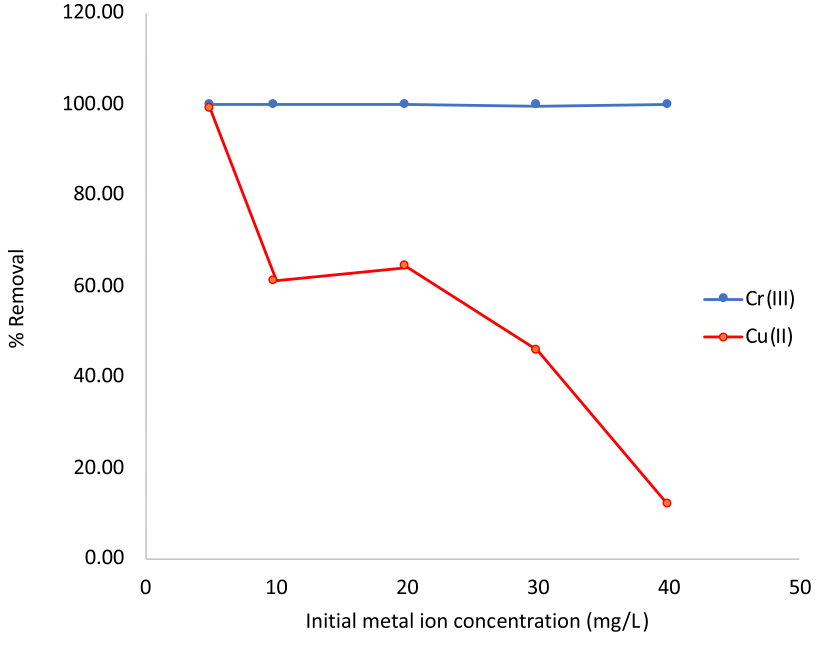

Figure 7. Effects of initial Concentrations of Cr (III) and Cu (II) on removal efficiency.

https://doi.org/10.1021/acsomega.3c08230
ACS Omega 2024, 9, 11500−11509

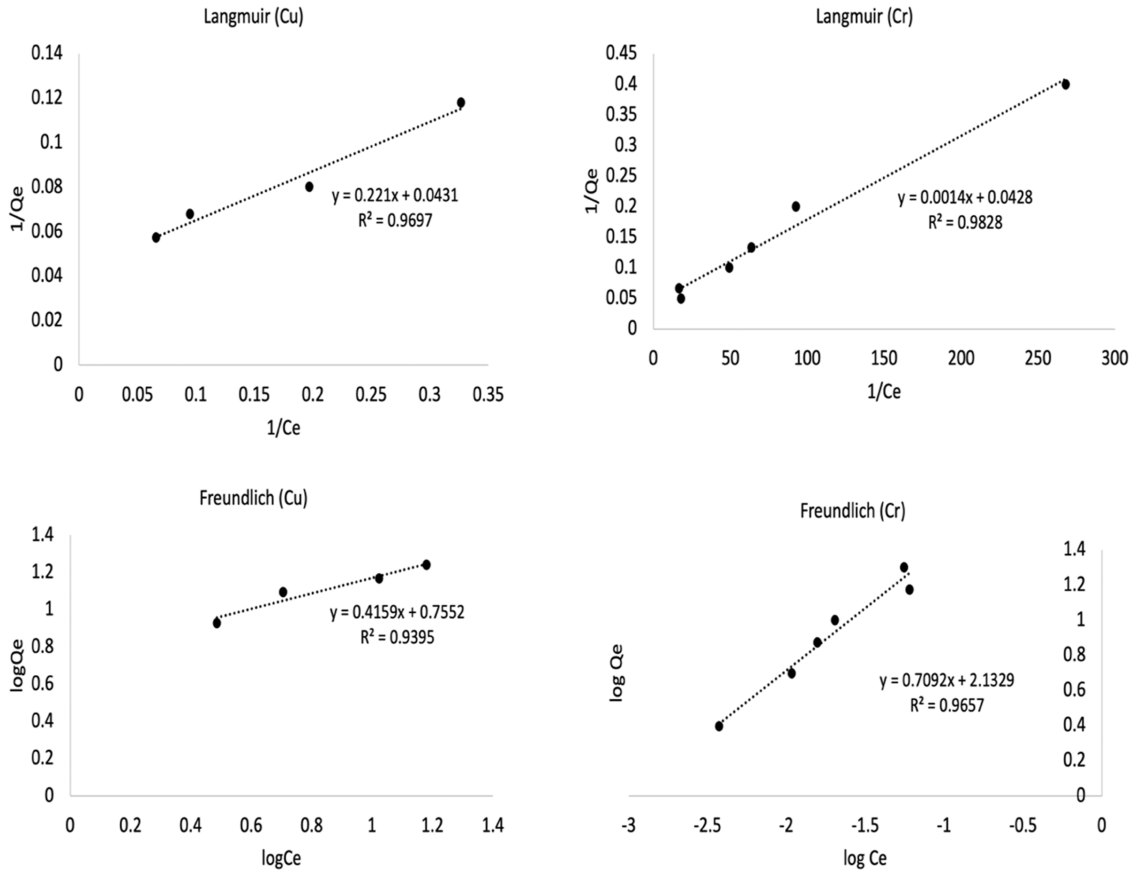

Figure 8. Equilibrium isotherms for the adsorption of Cr (III) and Cu (II) ions.

Table 2. Isotherm Modeling Data for the Removal of Cr (III) and Cu (II) by CDB

	Langmuir	
	Cr (III)	Cu (II)
q_{max} (mg/g)	23.3640	23.2010
K_L	30.5710	0.1950
R^2	0.9828	0.9697
	Freundlich	
	Cr (III)	Cu (II)
$1/n$	0.7092	0.4159
K_F	8.4390	2.1280
R^2	0.9657	0.9395

including Cr (III). Examination of the solutions employed in the study revealed an increase in the concentrations of Ca^{2+} and Mg^{2+} ions following the adsorption of Cr (III) ions. In a separate study focusing on the adsorption of Cu (II) by biochar derived from cow manure, results indicated a substantial reduction in the percentage content of K^+, Ca^{2+}, and Mg^{2+} after the adsorption of Cu (II) on the biochar, as evidenced by SEM-EDS readings.[5] SEM-EDX analysis of the CBD confirmed the presence of Ca^{2+}, Mg^{2+} cations on the surface of the biochar, providing additional support for the potential removal of Cu (II) and Cr (III) via a cation exchange mechanism. Further investigations will be conducted to ascertain the complete extent to which this mechanism contributed to the removal of Cr (III) and Cu (II) in this case.

In the removal of metal ions on biochar surfaces, the cation−π interaction assumes a critical role, particularly concerning positively charged metal cations such as copper Cu (II) and Cr (III). Biochar, containing aromatic carbon compounds with π-electron systems in the form of aromatic rings, serves as a favorable substrate for these types of interactions.[5] The cation−π mechanism involves electrostatic attraction between the positively charged metal ions and the π-electron cloud of the aromatic rings. This interaction enhances the binding affinity of metal ions to the biochar surface, contributing to the overall adsorption capacity. The aromatic rings, with their substantial π-electron clouds, offer specific and conducive sites for the formation of stable interactions with metal cations.[38] Research has consistently underscored the cation−π interaction as a credible mechanism for heavy metal adsorption across diverse biochar sources, including wood biochar, manure biochar, and sludge biochar.[39] In the case of camel dung biochar, FTIR scans identified distinctive peaks corresponding to C−H and C═C aromatic bonds, substantiating the likelihood of Cu (II)−π and Cr (III)−π interactions resulting from the adsorption of these metal ions on the biochar derived from camel dung.

The data in Table 3 demonstrates the promising adsorption capacity of camel dung biochar for both Cu (II) and Cr (III), positioning it competitively with other biochar materials made from plant and animal biomass. In comparison to dairy manure biochar, Ascophyllum nodosum (seaweed), and composted swine manure for Cu (II) adsorption, camel dung biochar demonstrates a noteworthy adsorption capacity of 23.20 mg/g, corresponding favorably with the reported values for other biochar materials in the table. Similarly, for Cr (III) adsorption, camel dung biochar exhibits a competitive adsorption capacity of 23.36 mg/g, comparable to biochar made from jackfruit peel and poultry manure, albeit lower than hornwort.

https://doi.org/10.1021/acsomega.3c08230
ACS Omega 2024, 9, 11500−11509

Table 3. Comparative Adsorptive Removal of Cu (II) and Cr (III) Using Plant and Animal Biomass

metal	adsorbent	kinetic model	isotherm model	adsorption capacity (mg/g)	references
Cu (II)	dairy manure biochar		L/F	54.4	11
	ascophyllum nodosum (seaweed)	PS2	L	53.19	33
	composted swine manure	PS2	SIPS	21.94	10
	camel dung biochar	PS2	L	23.20	this study
Cr (III)	jackfruit peel	PS2	L	13.50	37
	poultry manure biochar	PS2	F	34.00	3
	hornwort	PS2	L	60.20	4
	camel dung biochar	PS2	L	23.36	this study

To augment the adsorption capacity of camel dung biochar, future investigations may explore potential enhancements through various approaches, including surface activation techniques, alterations to pyrolysis conditions, and the incorporation of supplementary functional groups. These modifications are anticipated to offer promising pathways for refining the overall efficacy of camel dung biochar as a sustainable and potent adsorbent for the removal of heavy metals from aqueous solutions.

Recyclability Efficiency of CDB for Cr (III) and Cu (II). To maximize the potential use of the CDB, the solid adsorbent with adsorbed Cr (III) and Cu (II) was regenerated by washing with water. The regenerated CDB was reused for removal of Cr (III) and Cu (II), and the results obtained were 99.24 and 83.38% at first and second treatment for Cr (III) and 99.9 and 2.65% at first and second cycles for Cu (II), respectively. These findings demonstrate the high potential of CDB for Cr (III) even at extended treatment cycles. Conversely, a significant decrease in the removal efficiency of Cu (II) was observed in the second treatment cycle, and this could be possibly attributed to the strong binding of Cu (II) with CDB and less efficiency of the regeneration reagent. Prior research indicates that the binding of metal ions with the solid adsorbent and the regeneration solvent significantly influences reusability efficiency.[40] The leached concentrations of Cr (III) and Cu (II) were also analyzed after regeneration, and the results obtained showed that Cr (III) was leached at a slightly higher concentration (1.7% compared to 0.9%) than Cu (II). The high leaching of Cr (III) from CDB also depicts the possibility of greater adsorption sites for adsorption of metal at extended treatment cycles.

CONCLUSIONS

In summary, the multifaceted nature of the adsorption mechanisms, including complexation reactions, cation exchange, and π interactions, underscores the effectiveness of camel dung biochar as a versatile adsorbent for the removal of Cu (II) and Cr (III) ions from aqueous solutions. These findings provide valuable insights into the potential applications of biochar-based materials for heavy metal ion remediation in environmental and wastewater treatment processes. Additionally, minimizing the need for pH adjustment in water treatment processes that use CDB will reduce the consumption of chemicals and the generation of chemical waste. This supports the principles of sustainable and environmentally friendly practices, reducing the potential environmental impact associated with pH adjustment processes. Subsequent studies will be conducted to ascertain the biochar's reusability and leaching properties, along with an investigation into the influence of temperature on the efficacy of CDB as an adsorbent. The exploration of CDB's capacity to adsorb a broader spectrum of metal ions and organic contaminants will also be a focal point in forthcoming research efforts.

AUTHOR INFORMATION

Corresponding Author

Kenesha Wilson − *College of Natural and Health Sciences, Zayed University, Abu Dhabi, UAE;* orcid.org/0000-0002-8197-4477; Email: Kenesha.Wilson@zu.ac.ae

Authors

Jibran Iqbal − *College of Natural and Health Sciences, Zayed University, Abu Dhabi, UAE*

Amira Obaid Abdalla Obaid Hableel − *College of Natural and Health Sciences, Zayed University, Abu Dhabi, UAE*

Zainab Naji Khalaf Beyaha Alzaabi − *College of Natural and Health Sciences, Zayed University, Abu Dhabi, UAE*

Yousef Nazzal − *College of Natural and Health Sciences, Zayed University, Abu Dhabi, UAE*

Complete contact information is available at: https://pubs.acs.org/10.1021/acsomega.3c08230

Funding

This work was supported by Zayed University, Abu Dhabi, UAE under the Research Incentive Fund grant R21073.

Notes

The authors declare no competing financial interest.

ACKNOWLEDGMENTS

The authors would like to thank Dr. Cijo Xavier, Dr. Tony Myers, Mr. Ahmed Habreesh Alkatheeri, and Mr. Pramod Kumbhar for their invaluable contributions and unwavering support throughout this project.

REFERENCES

(1) Barakat, M. New trends in removing heavy metals from industrial wastewater. *Arabian J. Chem.* **2011**, *4* (4), 361−377.

(2) Gu, M.; Hao, L.; Wang, Y.; Li, X.; Chen, Y.; Li, W.; Jiang, L. The selective heavy metal ions adsorption of zinc oxide nanoparticles from dental wastewater. *Chem. Phys.* **2020**, *534*, No. 110750.

(3) Batool, S.; Idrees, M.; Al-Wabel, M. I.; Ahmad, M.; Hina, K.; Ullah, H.; Cui, L.; Hussain, Q. Sorption of Cr (III) from aqueous media via naturally functionalized microporous biochar: Mechanistic study. *Microchem. J.* **2019**, *144*, 242−253.

(4) Mokrzycki, J.; Michalak, I.; Rutkowski, P. Biochars obtained from freshwater biomass—green macroalga and hornwort as Cr (III) ions sorbents. *Biomass Convers. Biorefin.* **2021**, *11*, 301−313.

(5) Zhang, P.; Zhang, X.; Yuan, X.; Xie, R.; Han, L. Characteristics, adsorption behaviors, Cu (II) adsorption mechanisms by cow manure biochar derived at various pyrolysis temperatures. *Bioresour. Technol.* **2021**, *331*, No. 125013.

(6) Gupta, A.; Lutsenko, S. Human copper transporters: mechanism, role in human diseases and therapeutic potential. *Future Med. Chem.* **2009**, *1* (6), 1125−1142.

(7) Chen, T.; Zhou, Z.; Xu, S.; Wang, H.; Lu, W. Adsorption behavior comparison of trivalent and hexavalent chromium on biochar derived from municipal sludge. *Bioresour. Technol.* **2015**, *190*, 388−394.

(8) Qiu, Y.; Zhang, Q.; Gao, B.; Li, M.; Fan, Z.; Sang, W.; Hao, H.; Wei, X. Removal mechanisms of Cr (VI) and Cr (III) by biochar supported nanosized zero-valent iron: Synergy of adsorption, reduction and transformation. *Environ. Pollut.* **2020**, *265*, No. 115018.
(9) Wei, J.; Tu, C.; Yuan, G.; Liu, Y.; Bi, D.; Xiao, L.; Lu, J.; Theng, B. K.; Wang, H.; Zhang, L.; Zhang, X. Assessing the effect of pyrolysis temperature on the molecular properties and copper sorption capacity of a halophyte biochar. *Environ. Pollut.* **2019**, *251*, 56−65.
(10) Meng, J.; Feng, X.; Dai, Z.; Liu, X.; Wu, J.; Xu, J. Adsorption characteristics of Cu(II) from aqueous solution onto biochar derived from swine manure. *Environ. Sci. Pollut. Res. Int.* **2014**, *21* (11), 7035−7046. From NLM Medline.
(11) Xu, X.; Cao, X.; Zhao, L.; Wang, H.; Yu, H.; Gao, B. Removal of Cu, Zn, and Cd from aqueous solutions by the dairy manure-derived biochar. *Environ. Sci. Pollut. Res.* **2013**, *20* (1), 358−368.
(12) Wang, Y.; Liu, R. H2O2 treatment enhanced the heavy metals removal by manure biochar in aqueous solutions. *Sci. Total Environ.* **2018**, *628-629*, 1139−1148.
(13) Park, J. H.; Choppala, G. K.; Bolan, N. S.; Chung, J. W.; Chuasavathi, T. Biochar reduces the bioavailability and phytotoxicity of heavy metals. *Plant Soil* **2011**, *348* (1), 439−451.
(14) Wei, D.; Li, B.; Huang, H.; Luo, L.; Zhang, J.; Yang, Y.; Guo, J.; Tang, L.; Zeng, G.; Zhou, Y. Biochar-based functional materials in the purification of agricultural wastewater: fabrication, application and future research needs. *Chemosphere* **2018**, *197*, 165−180. Salem, I. B.; El Gamal, M.; Sharma, M.; Hameedi, S.; Howari, F. M. Utilization of the UAE date palm leaf biochar in carbon dioxide capture and sequestration processes. *J. Environ. Manage.* **2021**, *299*, No. 113644.
(15) Qin, J.; Qian, S.; Chen, Q.; Chen, L.; Yan, L.; Shen, G. Cow manure-derived biochar: Its catalytic properties and influential factors. *J. Hazard. Mater.* **2019**, *371*, 381−388.
(16) Mohan, D.; Sarswat, A.; Ok, Y. S.; Pittman, C. U., Jr Organic and inorganic contaminants removal from water with biochar, a renewable, low cost and sustainable adsorbent−a critical review. *Bioresour. Technol.* **2014**, *160*, 191−202.
(17) Xu, Y.; Qi, F.; Bai, T.; Yan, Y.; Wu, C.; An, Z.; Luo, S.; Huang, Z.; Xie, P. A further inquiry into co-pyrolysis of straws with manures for heavy metal immobilization in manure-derived biochars. *J. Hazard. Mater.* **2019**, *380*, No. 120870.
(18) Cuixia, Y.; Yingming, X.; Lin, W.; Xuefeng, L.; Yuebing, S.; Hongtao, J. Effect of different pyrolysis temperatures on physico-chemical characteristics and lead (II) removal of biochar derived from chicken manure. *RSC Adv.* **2020**, *10* (7), 3667−3674.
(19) Batool, S.; Idrees, M.; Hussain, Q.; Kong, J. Adsorption of copper (II) by using derived-farmyard and poultry manure biochars: Efficiency and mechanism. *Chem. Phys. Lett.* **2017**, *689*, 190−198.
(20) Chen, Z.-l.; Zhang, J.-q.; Huang, L.; Yuan, Z.-h.; Li, Z.-j.; Liu, M.-c. Removal of Cd and Pb with biochar made from dairy manure at low temperature. *J. Integr. Agric.* **2019**, *18* (1), 201−210.
(21) Animal Development and Health. United Arab Emirates Ministry of Climate Change and Environment, (accessed March 26, 2021), https://www.moccae.gov.ae/en/knowledge-and-statistics/wealth-and-animal-health.aspx. Livestock Statistics 2016. Federal Competitiveness and Statistics Centre, (accessed February 28, 2021) https://fcsc.gov.ae/en-us/Lists/D_StatisticsSubject/DispForm.aspx?ID=728).
(22) Westall, S. Camel dung fuels cement production in northern UAE. Reuters: 2019.
(23) Faye, B. *The Camel, New Challenges for a Sustainable Development*. Springer: 2016.
(24) Iqbal, J.; Shah, N. S.; Sayed, M.; Niazi, N. K.; Imran, M.; Khan, J. A.; Khan, Z. U. H.; Hussien, A. G. S.; Polychronopoulou, K.; Howari, F. Nano-zerovalent manganese/biochar composite for the adsorptive and oxidative removal of Congo-red dye from aqueous solutions. *J. Hazard. Mater.* **2021**, *403*, No. 123854.
(25) Uzun, B. B.; Apaydin-Varol, E.; Ateş, F.; Özbay, N.; Pütün, A. E. Synthetic fuel production from tea waste: characterisation of bio-oil and bio-char. *Fuel* **2010**, *89* (1), 176−184.
(26) Wang, S.; Kwak, J.-H.; Islam, M. S.; Naeth, M. A.; El-Din, M. G.; Chang, S. X. Biochar surface complexation and Ni (II), Cu (II), and Cd (II) adsorption in aqueous solutions depend on feedstock type. *Sci. Total Environ.* **2020**, *712*, No. 136538.
(27) Park, J.-H.; Cho, J.-S.; Ok, Y. S.; Kim, S.-H.; Kang, S.-W.; Choi, I.-W.; Heo, J.-S.; Delaune, R. D.; Seo, D.-C. Competitive adsorption and selectivity sequence of heavy metals by chicken bone-derived biochar: batch and column experiment. *J. Environ. Sci. Health, Part A* **2015**, *50* (11), 1194−1204.
(28) Nguyen, V. H.; Van, H. T.; Nguyen, V. Q.; Dam, X. V.; Hoang, L.; Ha, L. Magnetic Fe3O4 nanoparticle biochar derived from pomelo peel for reactive Red 21 adsorption from aqueous solution. *Journal of chemistry* **2020**, *2020*, No. 3080612, DOI: 10.1155/2020/3080612. Yao, S.; Li, X.; Cheng, H.; Zhang, C.; Bian, Y.; Jiang, X.; Song, Y. Resource utilization of a typical vegetable waste as biochars in removing phthalate acid esters from water: a sorption case study. *Bioresour. Technol.* **2019**, *293*, No. 122081.
(29) Li, M.; Lou, Z.; Wang, Y.; Liu, Q.; Zhang, Y.; Zhou, J.; Qian, G. Alkali and alkaline earth metallic (AAEM) species leaching and Cu (II) sorption by biochar. *Chemosphere* **2015**, *119*, 778−785.
(30) Khan, J. A.; Sayed, M.; Shah, N. S.; Khan, S.; Khan, A. A.; Sultan, M.; Tighezza, A. M.; Iqbal, J.; Boczkaj, G. Synthesis of N-doped TiO2 nanoparticles with enhanced photocatalytic activity for 2,4-dichlorophenol degradation and H2 production. *J. Environ. Chem. Eng.* **2023**, *11* (6), No. 111308.
(31) Yang, P.; Bai, W.; Zou, Y.; Zhang, X.; Yang, Y.; Duan, G.; Wu, J.; Xu, Y.; Li, Y. A melanin-inspired robust aerogel for multifunctional water remediation. *Mater. Horiz.* **2023**, *10* (3), 1020−1029.
(32) Hassan, M.; Naidu, R.; Du, J.; Liu, Y.; Qi, F. Critical review of magnetic biosorbents: Their preparation, application, and regeneration for wastewater treatment. *Sci. Total Environ.* **2020**, *702*, No. 134893.
(33) Kumar, P.; Patel, A. K.; Singhania, R. R.; Chen, C.-W.; Saratale, R. G.; Dong, C.-D. Enhanced copper (II) bioremediation from wastewater using nano magnetite (Fe3O4) modified biochar of Ascophyllum nodosum. *Bioresour. Technol.* **2023**, *388*, No. 129654.
(34) Al-Senani, G. M.; Al-Fawzan, F. F. Adsorption study of heavy metal ions from aqueous solution by nanoparticle of wild herbs. *Egypt. J. Aquat. Res.* **2018**, *44* (3), 187−194.
(35) Wang, F. Y.; Wang, H.; Ma, J. W. Adsorption of cadmium (II) ions from aqueous solution by a new low-cost adsorbent—Bamboo charcoal. *J. Hazard. Mater.* **2010**, *177* (1−3), 300−306.
(36) Mahdi, Z.; Yu, Q. J.; El Hanandeh, A. Investigation of the kinetics and mechanisms of nickel and copper ions adsorption from aqueous solutions by date seed derived biochar. *J. Environ. Chem. Eng.* **2018**, *6* (1), 1171−1181.
(37) Ranasinghe, S.; Navaratne, A.; Priyantha, N. Enhancement of adsorption characteristics of Cr (III) and Ni (II) by surface modification of jackfruit peel biosorbent. *J. Environ. Chem. Eng.* **2018**, *6* (5), 5670−5682.
(38) Yaphary, Y. L.; He, M.; Lu, G.; Zou, F.; Liu, P.; Tsang, D. C. W.; Leng, Z. Experiment and multiscale molecular simulations on the Cu absorption by biochar-modified asphalt: An insight into removal capability and mechanism of heavy metals from stormwater runoff. *Chem. Eng. J.* **2023**, *462*, No. 142205. Xu, Y.; Hu, J.; Zhang, X.; Yuan, D.; Duan, G.; Li, Y. Robust and multifunctional natural polyphenolic composites for water remediation. *Mater. Horiz.* **2022**, *9*, 187−194, DOI: 10.1039/D2MH00768A.
(39) Xu, D.; Zhao, Y.; Sun, K.; Gao, B.; Wang, Z.; Jin, J.; Zhang, Z.; Wang, S.; Yan, Y.; Liu, X.; Wu, F. Cadmium adsorption on plant-and manure-derived biochar and biochar-amended sandy soils: impact of bulk and surface properties. *Chemosphere* **2014**, *111*, 320−326.
(40) Lin, D.; Wu, F.; Hu, Y.; Zhang, T.; Liu, C.; Hu, Q.; Hu, Y.; Xue, Z.; Han, H.; Ko, T.-H. Adsorption of dye by waste black tea powder: parameters, kinetic, equilibrium, and thermodynamic studies. *J. Chem.* **2020**, *2020*, 1−13.

https://doi.org/10.1021/acsomega.3c08230
ACS Omega 2024, 9, 11500−11509